Measurement-induced criticality in random quantum circuits

Chao-Ming Jian,[1,2] Yi-Zhuang You,[3] Romain Vasseur,[4] and Andreas W. W. Ludwig[5]

[1]*Station Q, Microsoft Quantum, Santa Barbara, California 93106-6105, USA*
[2]*Kavli Institute of Theoretical Physics, University of California, Santa Barbara, California 93106, USA*
[3]*Department of Physics, University of California, San Diego, California 92093, USA*
[4]*Department of Physics, University of Massachusetts, Amherst, Massachusetts 01003, USA*
[5]*Department of Physics, University of California, Santa Barbara, California 93106, USA*

We investigate the critical behavior of the entanglement transition induced by projective measurements in (Haar) random unitary quantum circuits. Using a replica approach, we map the calculation of the entanglement entropies in such circuits onto a two-dimensional statistical-mechanics model. In this language, the area- to volume-law entanglement transition can be interpreted as an ordering transition in the statistical-mechanics model. We derive the general scaling properties of the entanglement entropies and mutual information near the transition using conformal invariance. We analyze in detail the limit of infinite on-site Hilbert space dimension in which the statistical-mechanics model maps onto percolation. In particular, we compute the exact value of the universal coefficient of the logarithm of subsystem size in the nth Rényi entropies for $n \geqslant 1$ in this limit using relatively recent results for the conformal field theory describing the critical theory of two-dimensional (2D) percolation, and we discuss how to access the generic transition at finite on-site Hilbert space dimension from this limit, which is in a universality class different from 2D percolation. We also comment on the relation to the entanglement transition in random tensor networks, studied previously in Vasseur *et al.* [Phys. Rev. B **100**, 134203 (2019)].

I. INTRODUCTION

Quantum entanglement plays a crucial role in modern condensed-matter physics, both in equilibrium and nonequilibrium settings. Under unitary evolution, the entanglement of generic isolated many-body quantum systems tends to increase to a volume-law scaling of the entanglement entropies of subsystems [1–9], as required by the eigenstate thermalization hypothesis [10,11] (ETH). It is then natural to ask whether different dynamical phases with different entanglement scaling can exist, and about the nature of the *entanglement transitions* separating these entanglement phases. An example of such an entanglement transition is provided by the many-body localization (MBL) transition [12–23], which occurs in the presence of random or quasiperiodic potentials, and separates the volume-law thermal dynamical phase from an area-law (nonthermal) MBL phase [24–31].

A completely different way to obtain an entanglement transition of a different kind between area- and volume-law states was introduced in Ref. [32]. There the transition was induced by tuning the bond dimension of a state obtained at the boundary of a two-dimensional random tensor network. This entanglement transition can be described by an effective two-dimensional statistical-mechanics model.

Shortly after, another type of entanglement transition was proposed using projective measurements: If a many-body quantum system is subjected to enough local measurements, such measurements can collapse the many-body wave function into an area-law entangled state, while with a low den-

sity of measurements, volume-law entanglement can survive. Such measurement-induced transitions in random unitary circuits [6,33–40] subjected to random local measurements were introduced in Refs. [41–43], and were studied numerically both for Haar and Clifford random gates. Despite the growing interest in this transition [44–48], it remains poorly understood, with the majority of results stemming from numerical observations. There have been only two exceptions: (i) A fine-tuned transition between area- and volume-law entangled phases was shown in Ref. [32] to be in the universality class of critical two-dimensional (2D) percolation described by an exactly solvable conformal field theory (CFT). This provided an existence proof for such a transition. Relaxing the fine-tuning induces a crossover to a transition in an analytically so-far not tractable universality class. (ii) Subsequently, the behavior of the zeroth Rényi entropy S_0 in the problem of the projective measurement-induced transition was mapped in Ref. [41] onto an exactly solvable "geometric" optimization problem for "minimal cuts" in 2D percolation. Since in the same reference critical behavior of the zeroth Rényi entropy S_0 was observed at a parameter value (probability of measurement) different from the one where all nth Rényi entropies S_n with $n \geqslant 1$ became critical, the significance of the minimal cut results for S_0 for the measurement-induced entanglement transition remains to be better understood.

In this paper, we provide a theory of the projective measurement-induced entanglement transition (with Haar random unitary gates) by mapping the calculation of entanglement entropies onto a statistical-mechanics model. Our

approach relies on a replica trick which allows us to deal with the intrinsic nonlinearities of projective measurements. The area- to volume-law entanglement transition then corresponds to an ordering transition in the statistical-mechanics model. This naturally explains the emergence of conformal invariance at the transition, and leads to universal scaling forms for the entanglement entropy and mutual information. In the limit of infinite on-site Hilbert space dimension $d = \infty$, we find that the entanglement transition is in the percolation universality class, and we compute the exact value of the universal coefficient of the logarithm of subsystem size in all nth Rényi entropies for $n \geqslant 1$ from the exactly known CFT, obtaining the value $=1/6$ for the entanglement of half of the system and open boundary conditions. This is in contrast to the value of the universal coefficient of the logarithm of subsystem size of the zeroth Rényi entropy computed in the same setting, as mentioned above, in Ref. [41] using the minimal cut method, which was found [49] in that work to be equal [44,50,51] to $= \ln 2 \times \sqrt{3}/(2\pi)$. [The latter quantity is $\approx \ln 2 \times 0.27 \approx 0.187$.] The fact that these two universal, exactly known numbers $1/6$ and $\ln 2 \times \sqrt{3}/(2\pi)$ are different appears to indicate that, while in the limit of infinite on-site Hilbert space dimension, the nth Rényi entropies for $n \geqslant 1$ and the zeroth Rényi entropy S_0 happen to become critical at the *same* parameter value (probability of measurement), they describe rather different and unrelated properties of the system. (This is in line with the observation, mentioned above, that these two quantities become critical at different parameter values in the generic case of *finite* on-site Hilbert space dimension.) The limit of an infinite on-site Hilbert space dimension also allows us to identify the generic transition for a finite on-site Hilbert space dimension as that generated by a crossover from the percolation conformal field theory by a single (renormalization group) relevant perturbation.

The remainder of this paper is organized as follows: In Sec. II, we introduce the model of random unitary circuits with random projective measurements, and explain how to compute the entanglement entropy using a replica approach. In Sec. III, we map the calculation of the entanglement entropy onto a statistical-mechanics model, and discuss the large d limit. Section IV describes the consequences of conformal invariance for scaling of various quantities for any d, while Sec. V addresses the $d = \infty$ limit in detail. Finally, Sec. VI deals with the nature of the transition at finite d and the close relation to the entanglement transition [32] in random tensor networks [32,52,53], and Sec. VII contains concluding remarks.

II. RANDOM QUANTUM CIRCUITS

We study the discrete-time dynamics of a 1D "qudit" chain. That is, each site of this 1D qudit chain has a local Hilbert space of dimension d. The discrete-time dynamics we focus on is generated by the quantum circuit with a "brick-wall" configuration shown in Fig. 1 that consists of random unitary operators and generalized measurements. In Fig. 1, the 1D qudit chain is along the x direction while the vertical direction represents time (or discrete time steps). Each green block represents an *independently Haar-random* two-site unitary
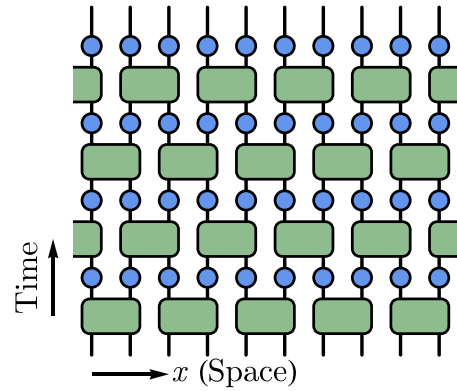

FIG. 1. Random unitary dynamics of a 1D qudit chain. The blue circles represent one-site generalized measurements, while the green blocks represent Haar-random two-site unitary gates that act on pairs of neighboring sites in the 1D qudit chain.

gate that acts on a pair of neighboring sites in the 1D qudit chain.

Each of the blue blocks represents a one-site generalized measurement. Such generalized measurements can be most conveniently described using the language of quantum channels [44,54], which we review in the following. In general, a quantum channel is a completely positive trace-preserving map, which can be described by a set $\mathcal{M} = \{M_\alpha\}$ of Kraus operators M_α (with $\alpha = 1, 2, \ldots$). The Kraus operators are normalized according to a generalized normalization condition $\sum_{M_\alpha \in \mathcal{M}} w(M_\alpha) M_\alpha^\dagger M_\alpha = \mathbb{1}$ with $w(M_\alpha)$ a non-negative real number for each Kraus operator $M_\alpha \in \mathcal{M}$, which is the weight of realizing M_α in the quantum channel. The left-hand side of this normalization condition can be viewed as the weighted sum of $M_\alpha^\dagger M_\alpha$'s with non-negative weights $w(M_\alpha)$. In the following, we will denote this weighted sum as $\mathbb{E}_{M_\alpha \in \mathcal{M}}$. For example, we can rewrite the generalized normalization condition as $\mathbb{E}_{M_\alpha \in \mathcal{M}} M_\alpha^\dagger M_\alpha = \sum_{M_\alpha \in \mathcal{M}} w(M_\alpha) M_\alpha^\dagger M_\alpha = \mathbb{1}$. Given the set $\mathcal{M}$ and the weights, the quantum channel is defined as the map from any density matrix ρ to $\mathbb{E}_{M_\alpha \in \mathcal{M}} M_\alpha \rho M_\alpha^\dagger$. In fact, in the standard definition of the Kraus operators and their normalization (see [54] for example), the weights $w(M_\alpha)$ are all taken to be 1. Here, we have made a generalization to nonunity weights and to the corresponding weighted sum for the convenience of later discussion. Given the set $\mathcal{M}$ (and the weights of the Kraus operators), the quantum channel can also be understood as a "probabilistic evolution." If one starts with a pure quantum state $|\psi\rangle$, for every Kraus operator $M_\alpha \in \mathcal{M}$, the quantum channel evolves $|\psi\rangle$ to $\frac{M_\alpha |\psi\rangle}{\|M_\alpha |\psi\rangle\|}$ with a probability of $w(M_\alpha) \|M_\alpha |\psi\rangle\|^2 = w(M_\alpha) \langle \psi | M_\alpha^\dagger M_\alpha | \psi \rangle$. Note that this probability is normalized due to the generalized normalization condition of the Kraus operators. Since we only consider one-site generalized measurements in the quantum circuit shown in Fig. 1, we then restrict the Kraus operators in $\mathcal{M}$ to be localized on the site where the corresponding blue block is acting.

The quantum channel description of generalized measurements can easily recover the standard projective measurement. For example, the one-site projective measurement with respect to a (orthonormal) set of basis vectors $|i\rangle$

(with $i = 1, 2, \ldots, d$) of the d-dimensional local Hilbert space on a given site can be described by the quantum channel with the set of Kraus operators $\mathcal{M}_1 = \{P_1, P_2, \ldots, P_d\}$ and the weights $w(P_i) = 1$ for $i = 1, 2, \ldots, d$. Here, $P_i = |i\rangle\langle i|$ is the projection operator on the ith basis vector. The quantum channel with the set $\mathcal{M}_1$ evolves (or collapses) a pure state $|\psi\rangle$ to $\frac{P_i|\psi\rangle}{\|P_i|\psi\rangle\|}$ with a probability of $w(P_i)\|P_i|\psi\rangle\|^2 = \|P_i|\psi\rangle\|^2$, which is as expected for the standard projective measurement.

Using the language of quantum channels, one can study more generalized forms of measurements. References [41] and [43] studied quantum circuits with $d = 2$ in similar configurations as Fig. 1 in which a quantum state, when it encounters a blue block in the quantum circuit, undergoes a standard one-site projective measurement with a classical probability p and stays intact with a classical probability $1 - p$. In this scenario, the associated quantum channel is described by the set of Kraus operators $\mathcal{M}_p = \{\mathbb{1}, P_1, P_2, \ldots, P_d\}$ equipped with the weights $w(\mathbb{1}) = 1 - p$ and $w(P_i) = p$ for $i = 1, 2, \ldots, d$. In the following sections, we also study this type of generalized measurement (or quantum channel) given by the set of Kraus operators $\mathcal{M}_p$ and the corresponding weights given above. We would also like to introduce a closely related generalized measurement given by the set of Kraus operators $\mathcal{M}'_p = \{\mathbb{1}\} \cup \{\sqrt{d}P_U | U \in \mathrm{U}(d)\}$ with $P_U \equiv U^\dagger P_1 U$, which is an (uncountable) infinite set. The subset $\{\sqrt{d}P_U | U \in \mathrm{U}(d)\}$ of $\mathcal{M}'_p$ is continuously parametrized by a (one-site) unitary matrix $U \in \mathrm{U}(d)$. The weight on the operator $\mathbb{1} \in \mathcal{M}'_p$ is still $1 - p$, which has the same physical interpretation as the weight of the operator $\mathbb{1}$ in $\mathcal{M}_p$. The weight on the infinite subset $\{\sqrt{d}P_U | U \in \mathrm{U}(d)\}$ is naturally given by the Haar measure: $w(\sqrt{d}P_U) = p\,dU$ where dU represents the Haar measure on $\mathrm{U}(d)$, normalized such that $\int_{U \in \mathrm{U}(d)} dU\, \mathbb{1} = \mathbb{1}$. The weighted sum of Kraus operators in $\mathcal{M}'_p$ is defined accordingly. For example, the generalized normalization condition of the Kraus operator is given by $\mathbb{E}_{M \in \mathcal{M}'_p} M^\dagger M = (1 - p)\mathbb{1}^\dagger \mathbb{1} + p \int_{U \in \mathrm{U}(d)} dU (\sqrt{d}P_U)^\dagger (\sqrt{d}P_U) = \mathbb{1}$. The relation between the generalized measurements defined by $\mathcal{M}_p$ and $\mathcal{M}'_p$ will be studied in the following section.

Before we focus on a specific choice of generalized measurements, let us rephrase the construction of the quantum circuit of interest to us in this paper using the quantum-channel language we introduced above. In a random quantum circuit of the configuration shown in Fig. 1, each green block is an independently Haar-random two-site unitary gate that acts on a pair of neighboring sites in the 1D qudit chain. Each of the blue blocks is independently and randomly drawn from the ensemble given by the set of Kraus operators $\mathcal{M}$ (and the associated weights) that is associated with the generalized measurement one wants to study. For each realization of the green and blue blocks, we can build a random quantum circuit, denoted as C, following Fig. 1. Such a quantum circuit evolves an initial pure state $|\psi\rangle$ of the 1D qudit chain to the pure state $\frac{C|\psi\rangle}{\|C|\psi\rangle\|}$. The probability for this evolution to occur is the product of three factors: (i) the squared norm $\|C|\psi\rangle\|^2 = \langle\psi|C^\dagger C|\psi\rangle = \mathrm{Tr}(C|\psi\rangle\langle\psi|C^\dagger)$, (ii) the weight for each Kraus operator in each blue block, and (iii) the Haar-measure probability for realizing each random two-site unitary gates in each green block. In [55], the evolution from $|\psi\rangle$ to $\frac{C|\psi\rangle}{\|C|\psi\rangle\|}$ is

also referred to as a *quantum trajectory*. Different realizations of the random quantum circuit C lead to different quantum trajectories.

We are interested in the average quantum dynamics induced by this random quantum circuit. We denote the average over all realizations of the random quantum circuit as $\mathbb{E}_C \cdots$. The precise meaning of $\mathbb{E}_C$ is the following. First, for each two-site random unitary gate (green block), $\mathbb{E}_C$ contains an independent integration over the Haar measure [of the $\mathrm{U}(d^2)$ group]. This integration will be denoted as $\mathbb{E}_U$ in the following. For each generalized measurement (blue block), $\mathbb{E}_C$ includes the weighted sum over the set of Kraus operators, $\mathbb{E}_\mathcal{M}$, as explained before.

One example of an averaged quantity under the quantum dynamics induced by this random quantum circuit is the averaged expectation value $\bar{\mathcal{O}}$ of an observable $\mathcal{O}$ in the state obtained from evolving the initial state $|\psi\rangle$ by the random quantum circuit:

$$
\begin{aligned}
\bar{\mathcal{O}} &= \mathbb{E}_C \left(\frac{\langle\psi|C^\dagger \mathcal{O} C|\psi\rangle}{\|C|\psi\rangle\|^2} \times \mathrm{Tr}(C|\psi\rangle\langle\psi|C^\dagger) \right) \\
&= \mathbb{E}_C \langle\psi|C^\dagger \mathcal{O} C|\psi\rangle,
\end{aligned} \tag{1}
$$

where $\frac{\langle\psi|C^\dagger \mathcal{O} C|\psi\rangle}{\|C|\psi\rangle\|^2}$ is the quantum-mechanical expectation value of the observable $\mathcal{O}$ in the state $\frac{C|\psi\rangle}{\|C|\psi\rangle\|}$, and the factor $\mathrm{Tr}(C|\psi\rangle\langle\psi|C^\dagger)$ is, as explained, one of the factors in the probability of the corresponding quantum trajectory. We see that Eq. (1) naturally agrees with the evolution of an observable $\mathcal{O}$ under a quantum channel (constructed from Fig. 1 by viewing each of the green and blue blocks as a quantum channel). The more interesting quantity we want to study is the (averaged) dynamics of subsystem entanglements under the random quantum circuit. Consider a subsystem A and its complement $\bar{A}$ of the 1D qudit chain. The nth Rényi entropy $S_{n,A}[|\psi\rangle]$ on the subsystem A of a pure state $|\psi\rangle$ follows the standard definition

$$
S_{n,A}[|\psi\rangle] = \frac{1}{1 - n} \ln \mathrm{Tr}_A \left(\rho_A^n \right), \tag{2}
$$

where $\rho_A = \mathrm{Tr}_{\bar{A}} |\psi\rangle\langle\psi|$ is the reduced density matrix on the subsystem A. Here, Tr_A (or $\mathrm{Tr}_{\bar{A}}$) represents the partial trace over the degrees of freedom in the subsystem A (or $\bar{A}$). Alternatively, $S_{n,A}[|\psi\rangle]$ in Eq. (2) can be expressed in terms of the expectation value of a permutation operator $\mathcal{S}_{n,A}$ acting on the the n-fold replicated state as

$$
S_{n,A}[|\psi\rangle] = \frac{1}{1 - n} \ln \mathrm{Tr}((|\psi\rangle\langle\psi|)^{\otimes n} \mathcal{S}_{n,A}), \tag{3}
$$

where $\mathcal{S}_{n,A}$ depends on the choice of entanglement region A and is defined as

$$
\mathcal{S}_{n,A} = \prod_x \mathcal{X}_{g_x}, \quad g_x = \begin{cases} (12\ldots n), & x \in A, \\ \text{identity} = e, & x \in \bar{A}. \end{cases} \tag{4}
$$

g_x labels the permutation on site x, and $\mathcal{X}_{g_x} = \sum_{[i]} |i_{g_x(1)} i_{g_x(2)} \ldots i_{g_x(n)}\rangle \langle i_1 i_2 \ldots i_n|$ is its representation on the replicated on-site Hilbert space, i.e., on its n-fold tensor product [56]. Here, as indicated in the equation above, g_x is the cyclic (identity) permutation when x is in the region A (when x is in the region $\bar{A}$). We are interested in the averaged

nth Rényi entropy $\bar{S}_{n,A}$ of the final state after the random quantum circuit evolution:

$$\bar{S}_{n,A} = \mathbb{E}_C S_{n,A}\left[\frac{C|\psi\rangle}{\|C|\psi\rangle\|}\right] \times \mathrm{Tr}(C|\psi\rangle\langle\psi|C^\dagger), \qquad (5)$$

$$
\begin{aligned}
\bar{S}_{n,A} &= \frac{1}{1-n}\mathbb{E}_C\left(\ln\frac{\mathrm{Tr}\left((C|\psi\rangle\langle\psi|C^\dagger)^{\otimes n}\mathcal{S}_{n,A}\right)}{\mathrm{Tr}(C|\psi\rangle\langle\psi|C^\dagger)^{\otimes n}}\right)\mathrm{Tr}(C|\psi\rangle\langle\psi|C^\dagger), \\
&= \lim_{m\to 0}\frac{1}{m(1-n)}\mathbb{E}_C\{[\mathrm{Tr}(C|\psi\rangle\langle\psi|C^\dagger)^{\otimes n}\mathcal{S}_{n,A}]^m - [\mathrm{Tr}(C|\psi\rangle\langle\psi|C^\dagger)^{\otimes n}]^m\}\,\mathrm{Tr}(C|\psi\rangle\langle\psi|C^\dagger), \\
&= \lim_{m\to 0}\frac{1}{m(1-n)}\mathbb{E}_C\,\mathrm{Tr}\left[(C|\psi\rangle\langle\psi|C^\dagger)^{\otimes nm+1}\left(\mathcal{S}_{n,A}^{\otimes m} - \mathbb{1}\right)\right],
\end{aligned}
\qquad (6)
$$

where we have introduced a second replica index m to resolve the ensemble average of the logarithm using $\ln x = \lim_{m\to 0}(x^{\otimes m}-1)/m$ and $\mathrm{Tr}(X^{\otimes m}) = (\mathrm{Tr}\,X)^m$. This replica trick was introduced in Ref. [32] in the context of random tensor networks, and in Ref. [38] for random unitary circuits. In this double replica scheme, the total number of replica is $Q = nm + 1$, and the replica limit $m \to 0$ corresponds to $Q \to 1$. As can be seen from Eq. (6), the additional replica apart from nm originated from the probability $\mathrm{Tr}(C|\psi\rangle\langle\psi|C^\dagger)$ of obtaining a measurement outcome. As a side comment, if we reweight this probability by a power q, i.e., replacing $\mathrm{Tr}(C|\psi\rangle\langle\psi|C^\dagger) \to \mathrm{Tr}(C|\psi\rangle\langle\psi|C^\dagger)^q$, we could also realize other replica limits, $Q = mn + q \to q$ as $m \to 0$.

To evaluate Eq. (6), we will need to calculate the ensemble average $\mathbb{E}_C\,C^{\otimes Q}\otimes C^{\dagger\otimes Q}$ of the tensor product of Q copies of the random quantum circuit C and Q copies of its conjugate $C^\dagger$. In the next section, we will show that the calculation of the average $\mathbb{E}_C\,C^{\otimes Q}\otimes C^{\dagger\otimes Q}$ can be mapped onto a statistical-mechanics model in $2 + 0$ dimensions. By imposing different boundary conditions corresponding to fixing permutations at the boundary [following Eq. (4)] to $\mathcal{S}_{n,A}^{\otimes m}$ or $\mathbb{1}$, the statistical-mechanics model results in different partition functions,

$$
\begin{aligned}
\mathcal{Z}_A &= \mathbb{E}_C\,\mathrm{Tr}\left[(C|\psi\rangle\langle\psi|C^\dagger)^{\otimes Q}\mathcal{S}_{n,A}^{\otimes m}\right], \\
\mathcal{Z}_\emptyset &= \mathbb{E}_C\,\mathrm{Tr}(C|\psi\rangle\langle\psi|C^\dagger)^{\otimes Q},
\end{aligned}
\qquad (7)
$$

from which the averaged nth Rényi entropy $\bar{S}_{n,A}$ can be obtained in the replica limit via

$$\bar{S}_{n,A} = \frac{n}{1-n}\lim_{Q\to 1}\frac{\mathcal{Z}_A - \mathcal{Z}_\emptyset}{Q-1}. \qquad (8)$$

Using the fact that $\mathcal{Z}_A = \mathcal{Z}_\emptyset = 1$ in the replica limit $m \to 0$ ($Q \to 1$), this can be rewritten in a more intuitive form as the free-energy cost of the domain wall associated with changing the boundary condition in the entanglement region:

$$\bar{S}_{n,A} = \lim_{m\to 0}\frac{F_A - F_\emptyset}{m(n-1)} = \lim_{m\to 0}\frac{\ln(\mathcal{Z}_A/\mathcal{Z}_\emptyset)}{m(1-n)}, \qquad (9)$$

with $F_A = -\ln\mathcal{Z}_A$ and $F_\emptyset = -\ln\mathcal{Z}_\emptyset$. Also, from the statistical-mechanics model perspective, we will see that the choice of the initial state $|\psi\rangle$ is not essential when the depth, namely the number of discrete time steps, of the random quantum circuit becomes large.

which can be rewritten as

III. STATISTICAL-MECHANICS MODEL

Let us derive the statistical-mechanics model for generic replica number Q first, before taking the replica limit $Q \to 1$. The evaluation of the expectation value $\mathbb{E}_C\,C^{\otimes Q}\otimes C^{\dagger\otimes Q}$ boils down to the ensemble average of the unitary gates and the generalized measurements in the circuit. Let U be a two-site Haar-random unitary gate. The average of the tensor product of Q identical copies of U and $U^\dagger$ under the Haar measure is given by (using standard graphical notations [57]):

$$(10)$$

where $\mathsf{Wg}_D(g)$ denotes the Weingarten function of the permutation g,

$$\mathsf{Wg}_D(g) = \frac{1}{Q!}\sum_{\lambda\vdash Q}\frac{\chi_\lambda(e)\chi_\lambda(g)}{\prod_{(i,j)\in Y(\lambda)}(D-i+j)}, \qquad (11)$$

where the sum is taken over all integer partitions λ of Q [denoted in the above equation by the notation $\lambda \vdash Q$, such that $\lambda = (\lambda_1, \lambda_2, \ldots)$ with $\lambda_1 \geqslant \lambda_2 \geqslant \cdots$, $\lambda_i \in \mathbb{N}$, and $\sum_i \lambda_i = Q$], and the product is taken over all cells (i, j) in the Young diagram $Y(\lambda)$ of the shape λ. Here e denotes the identity group element, and $\chi_\lambda(g)$ is the irreducible character of the symmetric group S_Q indexed by the partition λ.

As we average over all two-site unitary gates in the circuit, the partition function will break up into a product of independent contributions from the generalized measurements. Each generalized measurement is associated with the following partition function weight:

$$(12)$$

where M is an element of a set of Kraus operators. For $M = \mathbb{1}$, we have $W_{\mathbb{1}}(g_1, g_2) = \mathrm{Tr}\,\mathcal{X}_{g_1}\mathcal{X}_{g_2} = d^{|g_1^{-1}g_2|}$, where $|g|$ denotes [58] the number of cycles in the permutation g (including cycles of length 1). We consider two scenarios of the generalized measurement, described by the previously discussed
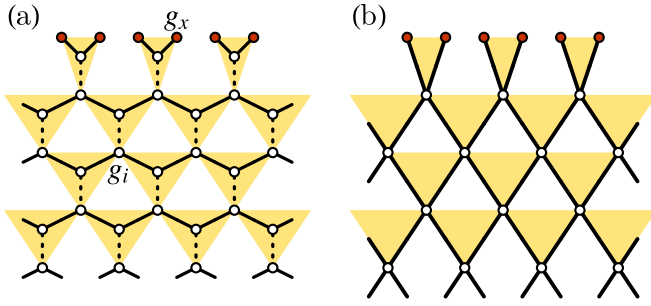
FIG. 2. (a) Geometry of the statistical-mechanics model of S_Q spins. The red sites correspond to the boundary spins to be pinned by the boundary condition. (b) In the $d = \infty$ limit, the model reduces to a Potts model on a square lattice.

sets of Kraus operators $\mathcal{M}_p$ and $\mathcal{M}'_p$, respectively. They lead to seemingly different ensemble averages:

$$\mathbb{E}_{M \in \mathcal{M}_p} W_M(g_1, g_2) = (1-p)d^{|g_1^{-1}g_2|} + pd, \quad (13)$$

$$\mathbb{E}_{M \in \mathcal{M}'_p} W_M(g_1, g_2) = (1-p)d^{|g_1^{-1}g_2|} + pd^Q. \quad (14)$$

However, in the replica limit $Q \to 1$, the two scenarios converge to the same partition function weight, although we emphasize that these factors can matter if one considers the limit $d \to \infty$ before the replica limit $Q \to 1$. We will take Eq. (14) for generic Q, and define the following weight function:

$$W_p(g) = (1-p)d^{|g|} + pd^Q, \quad (15)$$

which will be useful in constructing the Boltzmann weight of the following statistical-mechanics model.

Put together, the partition function $\mathcal{Z}_A$ in Eq. (7) can be formulated as a statistical-mechanics model on an anisotropic honeycomb lattice as depicted in Fig. 2(a) where a permutation group element $g_i \in S_Q$, a "spin," is defined on each site,

$$\mathcal{Z}_A = \sum_{\{g_i \in S_Q\}} \prod_{\langle ij \rangle \in \mathcal{E}_s} W_p(g_i^{-1}g_j) \prod_{\langle ij \rangle \in \mathcal{E}_d} \mathsf{Wg}_{d^2}(g_i^{-1}g_j), \quad (16)$$

and where $\mathcal{E}_s$ ($\mathcal{E}_d$) denotes the set of solid (dotted) links on the lattice. In connection with the original network geometry of the random circuit in Fig. 1, the vertical (dotted) links on the honeycomb lattice represent the Weingarten functions which originated from averaging the two-site unitary gates, and the zigzag (solid) links keep track of the contributions from the generalized measurements. In the following, we will refer to the model described by Eq. (16) as the "S_Q model," A similar statistical-mechanics model was derived in Ref. [38] for Haar random unitary circuits without projective measurements (i.e., $p = 0$). Here we generalized the model to the case with projective measurement.

We note a crucial symmetry property of the statistical-mechanics model that will become important in our discussion below, arising from the following symmetry of the local weights $W_p(g_i^{-1}g_j)$ and $\mathsf{Wg}_{d^2}(g_i^{-1}g_j)$ which enter the partition function in Eq. (16): They are invariant under global right and

left multiplication of all group elements,

$$g_i \to h_L g_i h_R^{-1}, \quad g_j \to h_L g_j h_R^{-1}, \quad \text{where } h_L, h_R \in S_Q. \quad (17)$$

This invariance follows from the fact that the Weingarten function in Eq. (11) as well as the "cycle-counting function" which appears in Eq. (15) and assigns to each permutation g the number of its cycles $|g|$, are both "class functions" (i.e., depend only the conjugacy class of the permutation group element).

The S_Q "spins" on the boundary, which are permutation group elements $g_x \in S_Q$ for boundary sites x, are pinned by the boundary condition, which is specified by the entanglement region A as follows:

$$g_x = \begin{cases} g_{\text{SWAP}} \equiv (12 \ldots n)^{\otimes m}, & x \in A, \\ \text{identity} = e, & x \in \bar{A}. \end{cases} \quad (18)$$

This equation follows from Eq. (4) by taking into account the m replica which arises, as discussed above, in addition to the Rényi replica from rewriting averages of the logarithm. By tuning the probability of measurement p, we can change the couplings on the solid links and drive, as we will see, an entanglement transition. As will be shown below, this measurement-induced transition can be naturally interpreted as a simple symmetry-breaking transition of the statistical-mechanics model.

In the limit where the on-site Hilbert space dimension $d = \infty$ is infinite, the S_Q model turns out to reduce to a Potts model with $Q!$ colors. To see this, we evaluate the partition function weight $J_p(g_i, g_j; g_k)$ associated with each down triangle (in yellow) in Fig. 2(a),

$$J_p(g_i, g_j; g_k) = \sum_{g_l \in S_Q} \; \boxed{\begin{array}{c} g_i \quad\quad g_j \\ g_l \\ g_k \end{array}}$$

$$= \sum_{g_l \in S_Q} W_p(g_i^{-1}g_l) W_p(g_j^{-1}g_l) \mathsf{Wg}_{d^2}(g_l^{-1}g_k) \quad (19)$$

The partition function in Eq. (16) can be equivalently written in terms of the triangle weight J_p as

$$\mathcal{Z}_A = \sum_{\{g_i \in S_Q\}} \prod_{\langle ijk \rangle \in \triangledown} J_p(g_i, g_j; g_k), \quad (20)$$

subject to the boundary condition that g_i should match g_x as specified in Eq. (18) on the boundary. Note that positivity of this weight is not guaranteed in general. For example $J_{p=0}((123), (132); e) = -2(d^2 - 1)/(d^6 + d^4 - 4d^2 - 4) < 0$ (for any realistic on-site Hilbert space dimension $d \geqslant 2$). This makes the statistical-mechanics nonunitary, which is not an issue for our approach, as the field theory describing the entanglement transition is necessarily nonunitary in any case because of the replica limit (see below). In the $d \to \infty$ limit, we obtain

$$\begin{aligned} W_p(g) &= d^Q[(1-p)\delta_g + p], \\ \mathsf{Wg}_{d^2}(g) &= d^{-2Q}\delta_g, \end{aligned} \quad (21)$$

where δ_g is the delta function that gives 1 if and only if $g = e$ is the identity element in the permutation group S_Q, and gives 0 otherwise. A detailed derivation of Eq. (21) can be found in the Appendix. Substituting Eq. (21) into Eq. (19), the triangle

weight reduces to

$$J_p(g_i, g_j; g_k) = \left[(1-p)\delta_{g_i^{-1}g_k} + p\right]\left[(1-p)\delta_{g_j^{-1}g_k} + p\right],$$
(22)

which further factorizes into partition function weights defined separately on the bonds $\langle ik \rangle$ and $\langle jk \rangle$. The partition function weight across the bond $\langle ik \rangle$ equals 1 if $g_i = g_k$ and p if $g_i \neq g_k$, and an analogous weight is assigned to the bond $\langle jk \rangle$. If we treat each on-site group element $g_i \in S_Q$ as a state (color) in a spin model, the partition function weight in Eq. (22) precisely matches that of a $Q!$-state Potts model on a square lattice, whose links are between sites i and k, and between sites i and j in each unit cell, as displayed in Fig. 2(b). By tuning the measurement rate p, the partition function $\mathcal{Z}_A$ in Eq. (20) undergoes a phase transition from the ordered phase (small p) to the disordered phase (large p) which we will analyze in detail below.

Away from the $d = \infty$ limit, the weight $W_p(g)$ receives the following leading corrections: $W_p(g) = d^Q[(1-p)\delta_g + p + \frac{1-p}{d}\delta'_g + \mathcal{O}(d^{-2})]$, where $\delta'_g = 1$ if g is a transposition such as, e.g., (12), and $\delta'_g = 0$ otherwise. The Weingarten function will not receive corrections at $1/d$ order. Using these results, the triangle weight can be evaluated to the $1/d$ order (see the Appendix for details), yielding

$$J_p(g_i, g_j; g_k) = \left[(1-p)\delta_{g_i^{-1}g_k} + p\right]\left[(1-p)\delta_{g_j^{-1}g_k} + p\right]$$
$$+ \frac{1-p}{d}\left[(1-p)\delta'_{g_i^{-1}g_j}\left(\delta_{g_i^{-1}g_k} + \delta_{g_j^{-1}g_k}\right)\right.$$
$$\left. + p\left(\delta'_{g_i^{-1}g_k} + \delta'_{g_j^{-1}g_k}\right)\right] + \mathcal{O}(d^{-2}).$$
(23)

Moreover, up to this order, we find that the weights of the S_Q model factorize into a product of weights associated with bonds of the same square lattice, depicted in Fig. 2(b), that appears in the $d = \infty$ result (22). Denoting the local weight on the bond $\langle ik \rangle$ as $e^{-E(g_i, g_k)}$, the energy function reads (see the Appendix)

$$E(g_i, g_k)$$
$$= -\ln\left[p + (1-p)\left(\delta_{g_i^{-1}g_k} + \frac{1}{d}\delta'_{g_i^{-1}g_k}\right) + \mathcal{O}(d^{-2})\right].$$
(24)

We see that, among all the domain walls, the $1/d$ corrections favor energetically transposition domain walls in our model, Eq. (20)—this will turn out to have important consequences in the following. Crucially, these $1/d$ corrections break the artificially large $S_{Q!}$ symmetry of the weights Eq. (22) of the $d \to \infty$ limit to the $S_Q \times S_Q$ symmetry present for finite d. Consequences of this reduction of symmetry by the $1/d$ corrections will be further analyzed below.

IV. CONFORMAL INVARIANCE

Now that we have mapped the calculation of the entanglement entropies of the random circuit with projective measurements onto a (replica) statistical-mechanics model, many qualitative features of the entanglement transition can be understood naturally. Our discussion follows closely Ref. [32] where a similar statistical-mechanics model was found to describe entanglement transitions in random tensor networks.

At small p, the Boltzmann weights give a ferromagnetic interaction favoring group elements (spins) on neighboring sites to be equal, and we thus expect an ordered phase of the statistical-mechanics model. In that phase, the free-energy cost $F_A - F_\emptyset$ in Eq. (9) associated with "twisting" the entanglement region scales with the size L_A of A at long times (many layers in the circuit), corresponding to volume-law entanglement $\bar{S}_{n,A} \sim L_A$ for sufficiently deep circuits (in the long-time limit $t \to \infty$). This is clearly the behavior expected without measurement, i.e., at $p = 0$. As the measurement rate p gets closer to 1, the effective temperature of the statistical-mechanics model is increased, leading to a disordered phase. The domain-wall condensate present in this phase can freely absorb the domain wall at the boundaries of the entanglement interval, such that, for a distance exceeding the correlation length from the boundary, there is no additional free-energy cost from the boundary domain. In this limit, the free-energy cost of the boundary domain will scale like the boundary of A, corresponding to area-law scaling of entanglement $\bar{S}_{n,A} \sim$ const.

The entanglement transition separating these two phases therefore corresponds to an ordering transition in the statistical-mechanics model. In general, assuming that the transition is of second order, it should be described by a two-dimensional conformal field theory (CFT) with central charge $c = 0$ in the replica limit $Q \to 1$. (Recall that c measures the way the free energy changes when a finite scale is introduced; since here the partition function $\mathcal{Z}_\emptyset = 1$ is trivial in the replica limit, we have $c = 0$.) Such CFTs at central charge $c = 0$ are nonunitary, and are notoriously hard to tackle even in two dimensions. Below we will propose a way to approach this transition from the infinite on-site Hilbert space size $d = \infty$ limit. Even without identifying the underlying CFT precisely, there are important consequences that can be deduced from conformal invariance alone.

First of all, since the bulk properties of the transition only depend on Q, the location of the bulk transition point at $p = p_c$ as well as all bulk critical exponents are the same for all Rényi entropies in the replica limit $Q \to 1$. (The Rényi entropies arise from observables located at the boundary of the system.) Our statistical model thus naturally explains why all Rényi entropies with $n \geqslant 1$ have a transition at the same value of p_c. (This was observed numerically in Ref. [41].)

Obviously, conformal invariance implies a dynamical critical exponent $z = 1$, so the scaling with time and space should be the same at the entanglement transition. To analyze the scaling of the entanglement entropy at the critical point, we note that the ratio of partition functions $\mathcal{Z}_A/\mathcal{Z}_\emptyset$ that appears in Eq. (9) corresponds in the CFT language to the two-point function of a boundary condition changing (BCC) operator [59,60] ϕ_{BCC}:

$$\mathcal{Z}_A/\mathcal{Z}_\emptyset = \langle \phi_{\mathrm{BCC}}(L_A)\phi_{\mathrm{BCC}}(0) \rangle,$$
(25)

where the operators are inserted at the boundary of the entanglement interval A. Near criticality, this two-point function scales as $\sim 1/L_A^{2h(n,m)} f_{n,m}(L_A/\xi_Q)$ with $\xi_Q \sim |p - p_c(Q)|^{-\nu(Q)}$ the correlation length of the statistical-mechanics model and $f_{n,m}$ are universal scaling functions that depend on n and m independently. Plugging this expression into the replica

formula (9), we find the general scaling of the entanglement entropy,

$$\bar{S}_{n,A} = \frac{2}{n-1} \left. \frac{\partial h}{\partial m} \right|_{m=0} \ln L_A + f_n \left(\frac{L_A}{\xi} \right), \qquad (26)$$

with $\xi \sim |p - p_c|^{-\nu}$ the correlation length in the limit $Q \to 1$. In particular, conformal invariance predicts that $\bar{S}_{n,A} \sim \ln L_A$ at criticality $p = p_c$, with a universal prefactor that depends on the Rényi index n. Note that Eq. (26) holds up to additive nonuniversal constants—in order to isolate the universal contributions, one can also take the derivative of $\bar{S}_{n,A}$ with respect to $\ln L_A$. This scaling form is in good agreement with the numerical observations of Refs. [41,42,44].

The BCC operator ϕ_{BCC} can also be used to derive the scaling of the mutual information of two regions $A = [x_1, x_2]$ and $B = [x_3, x_4]$: $\mathcal{I}_{A,B}^n = \bar{S}_{n,A} + \bar{S}_{n,B} - \bar{S}_{n,A \cup B}$, which maps naturally onto the four-point function of ϕ_{BCC}. As a result of conformal invariance, we find that the mutual information at criticality should depend only on the cross ratio [61]

$$\mathcal{I}_{A,B}^n = g_n(\eta) \text{ with } \eta = \frac{x_{12} x_{34}}{x_{13} x_{24}}, \qquad (27)$$

where $x_{ij} = \frac{L}{\pi} \sin \frac{\pi}{L} |x_i - x_j|$ for a system of size L with periodic boundary conditions. This scaling was checked numerically for Clifford unitary circuits in Ref. [44].

V. PERCOLATION LIMIT $d = \infty$

As we have shown above, the Boltzmann weights of the statistical model in the limit of infinite on-site Hilbert space dimension $d \to \infty$ take a very simple form, Eq. (22). This coincides with the high-temperature expansion of a Potts model with $Q!$ states on the square lattice, as an expansion onto the so-called Fortuin-Kasteleyn clusters [62] where an edge is occupied with weight $1 - p$, not occupied with weight p, and where each connected cluster (including single sites) carries a weight $Q!$—the number of Potts states. In the replica limit $Q \to 1$, this maps onto a bond percolation problem where $1 - p$ is the probability for a bond to be occupied. The partition function is trivial $\mathcal{Z}_\emptyset = 1$, and the transition occurs for $p_c = 1/2$. The correlation length diverges as $\xi \sim |p - p_c|^{-4/3}$ at the transition [63], and the central charge is $c = 0$ as expected from general considerations.

As just discussed, we have shown that the entanglement transition driven by projective measurements is in the universality class of 2D percolation ($Q \to 1$ limit of a $Q!$-Potts model). We note that based on earlier results on random unitary circuits without measurement at infinite on-site Hilbert space dimension [6,38], and based on the description obtained in Ref. [41] for the zeroth Renyi entropy in terms of a minimal cut classical optimization problem of paths in 2D percolation, it was conjectured in Ref. [41] that if the minimal cut classical optimization problem holds exactly in the projective measurement problem in the limit of infinite Hilbert space dimension d, then this optimization problem would also describe the nth Renyi entropies with $n \geqslant 1$, and not only the zeroth Renyi entropy S_0, with the same result. While Ref. [41] thus anticipated, based on these previous works, a connection of the projective measurement problem with percolation in the $d \to \infty$ limit, there are universal quantities that go beyond

this minimal cut picture and which can only be captured using a detailed analysis that relies on our replica trick formulation, as well as on detailed properties of the CFT describing the percolation critical point. In particular, we will show below that the $d = \infty$ limit requires a detailed knowledge of the CFT of 2D percolation, including very recent results [64], rather than merely a geometric "optimization problem" as in Ref. [41] for S_0.

To illustrate this point, we now provide an exact calculation of the universal prefactor of the logarithm in Eq. (26) in the limit $d \to \infty$. To do so, we need to identify the proper BCC operator in the $Q!$-state Potts CFT. This is actually a subtle point: Naively, this would appear to be the BCC operator which changes the boundary condition that is fixed to the identity permutation group element to the boundary condition that is fixed to the "SWAP" group element [second line of Eq. (18)] of the $Q!$-state Potts model in the percolation limit $Q \to 1$. It is well known that this BCC operator has finite scaling dimension $= 1/3$ in that limit [59,65,66]. This would imply an infinite limit for all Rényi entropies in Eq. (9) as $m \to 0$ using a power law in Eq. (25) with a finite decay exponent $= 2 \times 1/3$ in that limit.

This issue arises with this naive approach because the limit $d \to \infty$ was taken implicitly before the replica limit $Q \to 1$. To remedy this, the key idea is to "soften" the Boltzmann weights of the statistical-mechanics model in the vicinity of the boundary in a small "boundary layer" and replace them by those at a finite value of $1/d$. The bulk Boltzmann weights remain at $1/d = 0$, i.e., they are those of the Potts model. Since the Boltzmann weights of the boundary layer still favor "ferromagnetic" alignment of the S_Q-valued spins, the presence of the boundary layer does not modify the bias for boundary spins to align to the SWAP and the identity group elements, respectively, along segments A and $\bar{A}$ of the boundary. The effect of the boundary layer is that the "sharp" domain wall, where the group element along the boundary switches directly from identity to SWAP, splits [67] into a sequence of $m(n-1)$ consecutive "elementary" domain walls, each characterized by a single transposition having just one cycle of length 2 since domain walls with a single transposition are energetically favored by the finite-$1/d$ correction in the energy function Eq. (24). Using Eq. (24), it is straightforward to see that the energy cost of an elementary domain wall is $\Delta E_{\text{elementary}} = \ln p^{-1} - \frac{1-p}{p} d^{-1} + \mathcal{O}(d^{-2})$, which is lower than the energy cost of the domain wall separating the identity permutation from SWAP, which has energy $\Delta E_{\text{SWAP}} = \ln p^{-1} + \mathcal{O}(d^{-2})$. Note also that the total energy cost of an extended segment of the boundary separating uniform boundary conditions fixed to the identity on one side from uniform boundary conditions fixed to SWAP on the other of this segment, which consists of a sequence of $m(n-1)$ consecutive domain walls (whose group theory product must be equal to the SWAP group element), is also less than the cost of a sharp SWAP domain wall located on a single boundary link, since $m(n-1)\Delta E_{\text{elementary}} \ll \Delta E_{\text{SWAP}}$ in the replica limit $m \to 0$. Moreover, since the energy cost $\Delta E_{\text{elementary}}$ of a single transposition domain wall on a given boundary link is lower than that of a domain wall on the same link characterized by any other nonidentity permutation [using Eq. (24)], the sharp SWAP domain wall localized at a single

boundary link will split into $m(n-1)$ elementary domains walls, each localized on one of the $m(n-1)$ boundary links.

While the so-defined $(n-1)m$ elementary domain walls in the 2D Potts model can branch and touch each other, they are well-known and well-defined objects in the 2D Potts model, called "thin" domain walls, whose properties have recently been studied in great detail [64]. In our context the corresponding "split" BCC operator inserts $\ell = m(n-1)$ thin domain walls in the Potts theory. Using the results of Ref. [64], we find that this split BCC operator is $\Phi_{\text{BCC}} = \Phi_{2\ell-1,4\ell-1}$, using standard CFT notations[61,68]. Now, the $Q!$-state Potts model is described by a CFT [63,69] with central charge $c = 1 - \frac{6}{x(x+1)}$ and $x = \frac{\pi}{\arccos\frac{\sqrt{Q!}}{2}} - 1$. The scaling dimension of the boundary operator $\Phi_{r,s}$ is then $h_{r,s} = \frac{[(x+1)r - sx]^2 - 1}{4x(x+1)}$. The critical exponent $h_{2\ell-1,4\ell-1}$ vanishes as $\ell = m(n-1) \to 0$ in the replica limit $m \to 0$, as it should, and yields $\lim_{m\to 0} h_{2\ell-1,4\ell-1}/(n-1)m = 1/6$. In the replica limit, Eq. (26) therefore yields, for periodic spatial boundary conditions,

$$\bar{S}_{n,A} = \frac{1}{3}\ln L_A + \cdots, \tag{28}$$

and for open spatial boundary conditions,

$$\bar{S}_{n,A} = \frac{1}{6}\ln L_A + \cdots, \tag{29}$$

for all nth Rényi entropies $n \geq 1$ at criticality in the limit $d \to \infty$. (In the latter case these are represented by the one-point function of the split BCC operator.) We remark that our replica statistical-mechanics model only describes Rényi entropies with index $n \geq 1$, as quantities such as the domain-wall free energy all change sign at $n = 1$. While, as already mentioned above, Ref. [41] anticipated, based on previous works, a connection of the projective measurement problem with percolation in the $d \to \infty$ limit, we emphasize that the universal prefactor in Eq. (28) goes beyond the geometric minimal cut path optimization picture found in Ref. [41] to describe the zeroth Rényi entropy, and indicates a different behavior of the Rényi entropies $n \geq 1$. We also note that the universal prefactor of the logarithm in (28) and (29) is not purely a property of the 2D percolation CFT, as it depends on how this CFT is approached in the replica limit $m \to 0$—see (26).

We end by commenting that the same expression for the universal coefficient of the logarithm of subsystem size can be obtained in the random tensor network model of Ref. [32], when fine-tuned to the percolation critical point.

VI. GENERIC ENTANGLEMENT TRANSITION AT FINITE HILBERT SPACE DIMENSION d

In closing, we briefly comment on the CFT describing of the generic entanglement transition at finite Hilbert space dimension d. While the percolation limit $d \to \infty$ provides an in essence completely analytically tractable picture of the projective measurement-induced entanglement transition, this limit is not generic. The Potts model which is obtained in the limit $d \to \infty$ has a symmetry $S_{Q!}$, which is much larger than the $S_Q \times S_Q$ symmetry (corresponding to left/right multiplication) of the model (16) describing finite d. The leading operator in the $S_{Q!}$ Potts model that breaks the symmetry down

to $S_Q \times S_Q$ was identified in Ref. [32] as the so-called two-hull operator of the Potts model. In the replica percolation limit $Q \to 1$, this operator has scaling dimension $\Delta_{2-\text{hull}} = \frac{5}{4} < 2$ so it is relevant. (In fact, it turns out that this is the only renormalization-group relevant operator that can appear at the percolation fixed point, when the symmetry is broken to $S_Q \times S_Q$.) We therefore expect the finite d entanglement transition to be described by a different CFT, obtained as the IR fixed point of percolation perturbed by a two-hull operator. More precisely, let us work with the Landau-Ginzburg formulation of the $Q!$-state Potts field theory in terms of the Potts order parameter field ϕ_a with $a = 1, \ldots, Q!$, and $\sum_a \phi_a = 0$. The leading perturbation implementing the symmetry breaking $S_{Q!} \longrightarrow S_Q \times S_Q$ is given by [32]

$$\mathcal{L} = \mathcal{L}_{\text{Potts}} + \sum_{a,b \in S_Q} W(a^{-1}b)\phi_a\phi_b + \cdots, \tag{30}$$

where W is a class function of the permutation group S_Q. Crucially the labels a, b are now interpreted as elements of the group S_Q. The only allowed function $W(a^{-1}b)$ that would respect the $S_{Q!}$ symmetry is $W(a^{-1}b) = \delta_{a,b}$, but any class function of S_Q is enough to satisfy the $S_Q \times S_Q$ symmetry. The fate of this perturbed Potts model in the IR is currently unknown. However, we note that this field theory has exactly the same form as the one obtained for entanglement transitions in bulk random tensor networks in Ref. [32], as they both correspond to the symmetry breaking $S_{Q!} \longrightarrow S_Q \times S_Q$. It is therefore tempting to conjecture that they correspond to the same bulk universality class, although we caution that the two transitions correspond to different replica limits; $Q \to 1$ and $Q \to 0$ respectively, for the projective measurement transition studied in this work and for random tensor networks, respectively. In both cases, $Q! \to 1$ in the replica limit, so both problems correspond to a percolation theory perturbed by a two-hull operator. However, the different replica limits will likely yield different (trivial) prefactors, e.g., in Eq. (26).

VII. DISCUSSION

We have derived an exact statistical-mechanics model description of the entanglement transition that occurs in random unitary circuits with projective measurements [41,42]. Our approach relies on a replica trick that allows us to average entanglement entropies over the realizations of the random circuits and measurements, and to deal with the intrinsic non-linearities of the projective measurement problem. Our work naturally explains the emergence of conformal invariance at the entanglement transition, and predicts specific scaling forms for the entanglement entropy and mutual information. In the limit of infinite Hilbert space dimension $d = \infty$, we find that the transition is in the percolation universality class, and we computed the exact value of the universal coefficient of the logarithm of subsystem size in the nth Rényi entropies for $n \geq 1$. This limit also provides a natural starting point to identify the generic entanglement transition at finite Hilbert space dimension d, as a perturbation of percolation by a two-hull operator. Identifying the CFT in the generic case remains a challenging task for future work.

Note added. While we were finalizing this paper, a related work appeared on the ArXiv [70]. This work also derives a

statistical-mechanics model for the transition driven by weak measurements.

APPENDIX: 1/d EXPANSION

In this Appendix, we derive the $1/d$ expansion of the triangle weight in Eq. (19). Let $|g|$ be the number of cycles in the permutation g for $g \in S_Q$. We define the following group functions: δ_g and δ'_g,

$$\delta_g = \begin{cases} 1 & \text{if } |g| = Q, \text{ i.e., } g = e, \\ 0 & \text{otherwise}; \end{cases} \qquad \delta'_g = \begin{cases} 1 & \text{if } |g| = Q - 1, \text{ i.e., } g \text{ is a transposition,} \\ 0 & \text{otherwise}. \end{cases} \tag{A1}$$

Then the function $d^{|g|}$ can be expanded as

$$d^{|g|} = d^Q \delta_g + d^{Q-1} \delta'_g + \cdots = d^Q [\delta_g + d^{-1} \delta'_g + \mathcal{O}(d^{-2})]. \tag{A2}$$

With Eq. (A2), the weight function $W_p(g)$ in Eq. (15) admits the following expansion:

$$W_p(g) = (1-p)d^{|g|} + pd^Q = d^Q\left((1-p)\delta_g + p + \frac{1-p}{d}\delta'_g + \mathcal{O}(d^{-2})\right). \tag{A3}$$

The Weingarten function $\mathsf{Wg}_D(g)$ in Eq. (11) (with $D = d^2$) has an alternative definition that it is a class function satisfying the following equation:

$$\sum_{g_2 \in S_Q} \mathsf{Wg}_D(g_1^{-1}g_2) D^{|g_2^{-1}g_3|} = \delta_{g_1^{-1}g_3}. \tag{A4}$$

Given Eq. (A2), one can verify that the following expansion:

$$\mathsf{Wg}_D(g) = D^{-Q}[\delta_g - D^{-1}\delta'_g + \mathcal{O}(D^{-2})], \tag{A5}$$

is a solution of Eq. (A4) to the order of $1/D$, as

$$\sum_{g_2 \in S_Q} \mathsf{Wg}_D(g_1^{-1}g_2) D^{|g_2^{-1}g_3|} = \sum_{g_2 \in S_Q} \left[\delta_{g_1^{-1}g_2} - D^{-1}\delta'_{g_1^{-1}g_2} + \mathcal{O}(D^{-2})\right]\left[\delta_{g_2^{-1}g_3} + D^{-1}\delta'_{g_2^{-1}g_3} + \mathcal{O}(D^{-2})\right] = \delta_{g_1^{-1}g_3} + \mathcal{O}(D^{-2}). \tag{A6}$$

Using Eqs. (A3) and (A5), we can now evaluate the $1/d$ expansion for the triangle weight $J(g_i, g_j; g_k)$,

$$J_p(g_i, g_j; g_k) = \sum_{g_l \in S_Q} W_p(g_i^{-1}g_l) W_p(g_j^{-1}g_l) \mathsf{Wg}_{d^2}(g_l^{-1}g_k) = \sum_{g_l \in S_Q} d^Q\left((1-p)\delta_{g_i^{-1}g_l} + p + \frac{1-p}{d}\delta'_{g_i^{-1}g_l} + \mathcal{O}(d^{-2})\right)$$

$$\times d^Q\left((1-p)\delta_{g_j^{-1}g_l} + p + \frac{1-p}{d}\delta'_{g_j^{-1}g_l} + \mathcal{O}(d^{-2})\right) d^{-2Q}\left(\delta_{g_l^{-1}g_k} - d^{-2}\delta'_{g_l^{-1}g_k} + \mathcal{O}(d^{-4})\right)$$

$$= \left((1-p)\delta_{g_i^{-1}g_k} + p\right)\left((1-p)\delta_{g_j^{-1}g_k} + p\right) + \left((1-p)\delta_{g_i^{-1}g_k} + p\right)\frac{1-p}{d}\delta'_{g_j^{-1}g_k}$$

$$+ \left((1-p)\delta_{g_j^{-1}g_k} + p\right)\frac{1-p}{d}\delta'_{g_i^{-1}g_k} + \mathcal{O}(d^{-2})$$

$$= \left((1-p)\delta_{g_i^{-1}g_k} + p\right)\left((1-p)\delta_{g_j^{-1}g_k} + p\right) + \frac{1-p}{d}\left((1-p)\delta'_{g_i^{-1}g_j}\left(\delta_{g_i^{-1}g_k} + \delta_{g_j^{-1}g_k}\right) + p\left(\delta'_{g_j^{-1}g_k} + \delta'_{g_i^{-1}g_k}\right)\right) + \mathcal{O}(d^{-2}). \tag{A7}$$

The result matches Eqs. (22) and (23) as claimed in the main text.

To the same order $\mathcal{O}(d^{-2})$, this triangle weight can be rewritten as a product of Boltzmann weight on the links of the square lattice in Fig. 2 (b):

$$J_p(g_i, g_j; g_k) = \left((1-p)\delta_{g_i^{-1}g_k} + p + \frac{1-p}{d}\delta'_{g_i^{-1}g_k}\right)\left((1-p)\delta_{g_j^{-1}g_k} + p + \frac{1-p}{d}\delta'_{g_j^{-1}g_k}\right) + \mathcal{O}(d^{-2}). \tag{A8}$$

This can be checked by expanding the product explicitly and using the identity $\delta_{g_i^{-1}g_k}\delta'_{g_j^{-1}g_k} = \delta_{g_i^{-1}g_k}\delta'_{g_j^{-1}g_i}$. Therefore, at this order, the weights of the S_Q model can be factorized into a product of local weights over links of the square lattice, that we rewrite as $e^{-E(g_i,g_k)}$, with the energy function

$$E(g_i, g_k) = -\ln\left[p + (1 - p)\left(\delta_{g_i^{-1}g_k} + \frac{1}{d}\delta'_{g_i^{-1}g_k}\right) + \mathcal{O}(d^{-2})\right]. \tag{A9}$$

[1] P. Calabrese and J. Cardy, J. Stat. Mech.: Theory Exp. (2005) P04010.

[2] H. Kim and D. A. Huse, Phys. Rev. Lett. **111**, 127205 (2013).

[3] H. Liu and S. J. Suh, Phys. Rev. Lett. **112**, 011601 (2014).

[4] A. M. Kaufman, M. E. Tai, A. Lukin, M. Rispoli, R. Schittko, P. M. Preiss, and M. Greiner, Science **353**, 794 (2016).

[5] W. W. Ho and D. A. Abanin, Phys. Rev. B **95**, 094302 (2017).

[6] A. Nahum, J. Ruhman, S. Vijay, and J. Haah, Phys. Rev. X **7**, 031016 (2017).

[7] C. Jonay, D. A. Huse, and A. Nahum, arXiv:1803.00089.

[8] B. Bertini, P. Kos, and T. Prosen, Phys. Rev. X **9**, 021033 (2019).

[9] D. E. Parker, X. Cao, A. Avdoshkin, T. Scaffidi, and E. Altman, Phys. Rev. X **9**, 041017 (2019).

[10] J. M. Deutsch, Phys. Rev. A **43**, 2046 (1991).

[11] M. Srednicki, Phys. Rev. E **50**, 888 (1994).

[12] D. J. Luitz, N. Laflorencie, and F. Alet, Phys. Rev. B **91**, 081103(R) (2015).

[13] J. A. Kjäll, J. H. Bardarson, and F. Pollmann, Phys. Rev. Lett. **113**, 107204 (2014).

[14] R. Vosk, D. A. Huse, and E. Altman, Phys. Rev. X **5**, 031032 (2015).

[15] A. C. Potter, R. Vasseur, and S. A. Parameswaran, Phys. Rev. X **5**, 031033 (2015).

[16] M. Serbyn, Z. Papić, and D. A. Abanin, Phys. Rev. X **5**, 041047 (2015).

[17] V. Khemani, S. P. Lim, D. N. Sheng, and D. A. Huse, Phys. Rev. X **7**, 021013 (2017).

[18] M. Schreiber, S. S. Hodgman, P. Bordia, H. P. Lüschen, M. H. Fischer, R. Vosk, E. Altman, U. Schneider, and I. Bloch, Science **349**, 842 (2015).

[19] P. T. Dumitrescu, R. Vasseur, and A. C. Potter, Phys. Rev. Lett. **119**, 110604 (2017).

[20] T. Thiery, F. Huveneers, M. Müller, and W. De Roeck, Phys. Rev. Lett. **121**, 140601 (2018).

[21] L. Zhang, B. Zhao, T. Devakul, and D. A. Huse, Phys. Rev. B **93**, 224201 (2016).

[22] A. Goremykina, R. Vasseur, and M. Serbyn, Phys. Rev. Lett. **122**, 040601 (2019).

[23] P. T. Dumitrescu, A. Goremykina, S. A. Parameswaran, M. Serbyn, and R. Vasseur, Phys. Rev. B **99**, 094205 (2019).

[24] D. M. Basko, I. L. Aleiner, and B. L. Altshuler, Ann. Phys. **321**, 1126 (2006).

[25] V. Oganesyan and D. A. Huse, Phys. Rev. B **75**, 155111 (2007).

[26] A. Pal and D. A. Huse, Phys. Rev. B **82**, 174411 (2010).

[27] B. Bauer and C. Nayak, J. Stat. Mech.: Theory Exp. (2013) P09005.

[28] M. Serbyn, Z. Papić, and D. A. Abanin, Phys. Rev. Lett. **111**, 127201 (2013).

[29] D. A. Huse, R. Nandkishore, and V. Oganesyan, Phys. Rev. B **90**, 174202 (2014).

[30] R. Nandkishore and D. A. Huse, Annu. Rev. Condens. Matter Phys. **6**, 15 (2015).

[31] D. A. Abanin, E. Altman, I. Bloch, and M. Serbyn, Rev. Mod. Phys. **91**, 021001 (2019).

[32] R. Vasseur, A. C. Potter, Y.-Z. You, and A. W. W. Ludwig, Phys. Rev. B **100**, 134203 (2019).

[33] A. Nahum, S. Vijay, and J. Haah, Phys. Rev. X **8**, 021014 (2018).

[34] C. W. von Keyserlingk, T. Rakovszky, F. Pollmann, and S. L. Sondhi, Phys. Rev. X **8**, 021013 (2018).

[35] A. Chan, A. De Luca, and J. T. Chalker, Phys. Rev. X **8**, 041019 (2018).

[36] A. Chan, A. De Luca, and J. T. Chalker, Phys. Rev. Lett. **121**, 060601 (2018).

[37] T. Rakovszky, F. Pollmann, and C. W. von Keyserlingk, Phys. Rev. X **8**, 031058 (2018).

[38] T. Zhou and A. Nahum, Phys. Rev. B **99**, 174205 (2019).

[39] V. Khemani, A. Vishwanath, and D. A. Huse, Phys. Rev. X **8**, 031057 (2018).

[40] A. J. Friedman, A. Chan, A. De Luca, and J. T. Chalker, Phys. Rev. Lett. **123**, 210603 (2019).

[41] B. Skinner, J. Ruhman, and A. Nahum, Phys. Rev. X **9**, 031009 (2019).

[42] Y. Li, X. Chen, and M. P. A. Fisher, Phys. Rev. B **98**, 205136 (2018).

[43] A. Chan, R. M. Nandkishore, M. Pretko, and G. Smith, Phys. Rev. B **99**, 224307 (2019).

[44] Y. Li, X. Chen, and M. P. A. Fisher, Phys. Rev. B **100**, 134306 (2019).

[45] S. Choi, Y. Bao, X.-L. Qi, and E. Altman, arXiv:1903.05124.

[46] M. Szyniszewski, A. Romito, and H. Schomerus, Phys. Rev. B **100**, 064204 (2019).

[47] M. J. Gullans and D. A. Huse, arXiv:1905.05195.

[48] Q. Tang and W. Zhu, Phys. Rev. Res. **2**, 013022 (2020).

[49] While in Ref. [41] all entanglement entropies are measured in units of ln 2 (the logarithm of the on-site Hilbert space dimension), in the present work they are measured in units of (ln e) = 1. For this reason, in order to compare values of entanglement entropies, those obtained in Ref. [41] have to be multiplied by a factor of ln 2 in order to compare them with those in the present paper.

[50] J. Jiang and C.-L. You, Stoch. Process. Appl. **129**, 2049 (2019).

[51] Reference [41] states that the minimal cut optimization problem corresponds precisely to "first passage percolation." Reference [44] identified Ref. [50] that computed exactly the corresponding quantity in first passage percolation language, leading to the statement that the exact value of the 0th Renyi entropy measured

in units of ln 2 is exactly $[\sqrt{3}/(2\pi)]$. The latter value agrees with 0.27, numerically obtained in Ref. [41].

[52] P. Hayden, S. Nezami, X.-L. Qi, N. Thomas, M. Walter, and Z. Yang, J. High Energy Phys. 11 (2016) 009.

[53] X.-L. Qi, Z. Yang, and Y.-Z. You, J. High Energy Phys. 08 (2017) 060.

[54] M. A. Nielsen and I. L. Chuang, *Computation and Quantum Information* (Cambridge University Press, Cambridge, UK, 2010).

[55] H. M. Wiseman, Quantum Semiclass. Opt. **8**, 205 (1996).

[56] An orthonormal basis of which is denoted by $|i_1, i_2, \ldots, i_n\rangle = |i_1\rangle \otimes |i_2\rangle \otimes \cdots \otimes |i_n\rangle$.

[57] R. Orús, Ann. Phys. **349**, 117 (2014).

[58] The quantity $|g|$ was denoted in [32] by the symbol $C(g)$. The quantity $(|e| - |g|)$, where e denotes the identity permutation, equals the minimal number of transpositions necessary to represent the permutation g as a product of transpositions.

[59] J. L. Cardy, Nucl. Phys. B **240**, 514 (1984).

[60] J. Cardy, *Encyclopedia of Mathematical Physics* (Academic Press, Oxford, 2006), pp. 333–340.

[61] P. Francesco, P. Mathieu, and D. Sénéchal, *Conformal Field Theory* (Springer-Verlag, New York, 1997).

[62] C. Fortuin and P. Kasteleyn, Physica **57**, 536 (1972).

[63] J. L. Black and V. J. Emery, Phys. Rev. B **23**, 429 (1981).

[64] J. Dubail, J. L. Jacobsen, and H. Saleur, J. Stat. Mech.: Theory Exp. (2010) P12026.

[65] J. L. Cardy, Nucl. Phys. B **324**, 581 (1989).

[66] J. L. Cardy, J. Phys. A: Math. Gen. **25**, L201 (1992).

[67] The notion of splitting of domains walls characterized by permutation group elements was previously discussed in the different context of entanglement in many-body chaotic *unitary* Haar random circuits, without measurements, in [38].

[68] More precisely, we identify Φ_{BCC} as the most relevant operator in the fusion of the "fixed/fixed" BCC operator $\Phi_{1,3}$ with $\Phi_{1+2(\ell-1),1+4(\ell-1)}$. The latter operator inserts $\ell - 1$ domain walls (since $\Phi_{1,3}$ already insert one domain wall) with otherwise free boundary conditions, as introduced in Ref. [64].

[69] M. den Nijs, Phys. Rev. B **27**, 1674 (1983).

[70] Y. Bao, S. Choi, and E. Altman, Phys. Rev. B **101**, 104301 (2020).